Forschungszentrum Karlsruhe
in der Helmholtz-Gemeinschaft

Wissenschaftliche Berichte

FZKA 7525

New Treatment of the Conversion $\gamma \to \mu^+ + \mu^-$ in CORSIKA

D. Heck

Institut für Kernphysik

Dezember 2009

Forschungszentrum Karlsruhe

in der Helmholtz-Gemeinschaft

Wissenschaftliche Berichte

FZKA 7525

New Treatment of the Conversion $\gamma \to \mu^+ + \mu^-$ in CORSIKA

D. Heck

Institut für Kernphysik

Forschungszentrum Karlsruhe GmbH, Karlsruhe
2009

Forschungszentrum Karlsruhe GmbH
Postfach 3640, 76021 Karlsruhe

Mitglied der Hermann von Helmholtz-Gemeinschaft
Deutscher Forschungszentren (HGF)

ISSN 0947-8620

urn:nbn:de:0005-075251

Abstract

New Treatment of the conversion $\gamma \rightarrow \mu^+ + \mu^-$ in CORSIKA

This report describes the new treatment of the conversion of gamma rays into a muon pair $\gamma \rightarrow \mu^+ + \mu^-$ in the air shower simulation program CORSIKA. The physics background of the new treatment is given, the resulting muon properties of old and new treatments are compared and the differences in muons from air showers of $E_0 = 10^{19}$ eV arriving at the detector level are discussed.

Zusammenfassung

Neue Behandlung der Konversion $\gamma \rightarrow \mu^+ + \mu^-$ in CORSIKA

Dieser Bericht beschreibt die neue Behandlung der Konversion von Gammastrahlung in ein Myonenpaar $\gamma \rightarrow \mu^+ + \mu^-$ in dem Luftschauer-Simulationsprogramm CORSIKA. Der physikalische Hintergrund der neuen Behandlung wird erläutert, die resultierenden Myon-Eigenschaften der alten und neuen Behandlung werden verglichen und die Differenzen der Myonen aus Luftschauern von $E_0 = 10^{19}$ eV, die am Beobachtungsniveau ankommen, werden diskutiert.

Contents

1 Introduction

Already in the first versions of CORSIKA [1] the conversion of a gamma into a muon pair had been implemented. For simplicity this implementation treated the $\gamma \to \mu^+ + \mu^-$ conversion in full analogy with the $\gamma \to e^+ + e^-$ pair production process, just replacing the electron rest mass by that of the muon. The resulting cross section looked similar to that published by Stanev & Vankov [2] but shifted by a factor of about 200 to lower energies. In 1999 (after publication of the CORSIKA physics description [3]) this energy shift was eliminated by replacing correctly in the PEGS4 [4] cross section calculation program not only the electron mass by the muon mass, but also the Compton wavelength of the electron by that of the muon.

Recently A. Ò Murchadha [5] brought my attention to the publication of Burkhardt et al. [6] demonstrating that the rise in the $\gamma \to \mu^+ + \mu^-$ conversion cross section in air starts already at lower energies. The reason for the different behavior will be explained in the next section which presents also the resulting cross section. The more precise sampling leads to a slightly different energy distribution of the produced muons as discussed in Sect. 3 and especially to a much wider distribution of the polar angles as shown in Sect. 4. In Sect. 5 the muon energy spectra from air showers produced with the old an new method are compared. Other rare muon production processes are discussed in Sect. 6 without taking them into account in CORSIKA, and in Sect. 7 this report is concluded with final remarks.

2 Improved Treatment of Screening

The conversion of a gamma into two leptons is only possible in the presence of an electric Coulomb field of a nucleus to provide simultaneously the exact conservation of energy and momentum. The conversion might be explained by the existence of a virtual photon which transfers the required momentum from the participating nucleus. With increasing energy of the primary gamma the transferred momentum and hence the energy of this virtual photon decreases. This is equivalent with a larger minimal distance to the nucleus at which the gamma may produce a lepton pair. Thus with increasing primary gamma energy equivalent with a larger possible impact parameter the cross section increases. But as the atomic nucleus is shielded by the atomic electrons, the cross section will not grow to infinity, rather it saturates when the impact parameter exceeds the outer diameter of the electron cloud which surrounds the nucleus and screens its field for larger radii. This effect is described by the screening parameter $\delta \sim r_Z / R_{max}$, which is essentially the ratio of the radius of the atomic cloud r_Z and the maximum impact parameter R_{max}.

In the case of large gamma energies $E_\gamma \gg m_l$ compared to the mass m_l of the created leptons, the minimum necessary momentum transfer q_{min} from the nucleus is

$$q_{min} = \frac{m_l^2 \, E_\gamma}{2 \, E_+ E_-} \, ,$$

where E_+ and E_- are the energies of the created leptons. With the Heisenberg uncertainty relation we get from this minimum momentum the maximal distance

$$R_{max} \sim \frac{\hbar}{q_{min}} = \frac{\hbar\, 2\, E_+ E_-}{m_l^2\, E_\gamma} \,.$$

The effective radius r_Z of an atom with atomic number Z is given by the Thomas-Fermi model to

$$r_Z = \frac{\hbar^2}{m_e\, e^2}\, Z^{-1/3} \,.$$

With these relations and the definition of the fine structure constant $\alpha = e^2/4\,\pi\,\hbar$ we can rewrite the screening parameter δ to

$$\delta \sim \frac{r_Z}{R_{max}} = \frac{m_l^2\, E_\gamma}{2\, E_+ E_- (\alpha\, m_e\, Z^{1/3})} \,.$$

The screening parameter increases quadratically with the mass of the produced lepton pair. The saturation in the cross section therefore increases from ~ 10 GeV for e^+e^- pairs to more than ~ 100 TeV for $\mu^+\mu^-$ pairs. This behavior was already correctly implemented in the old treatment (1999) of the $E_\gamma \rightarrow \mu^+ + \mu^-$ conversion.

But there is another feature which was incorrect in the old treatment: In the calculation of the cross section the integration over the form factor of the atom has to

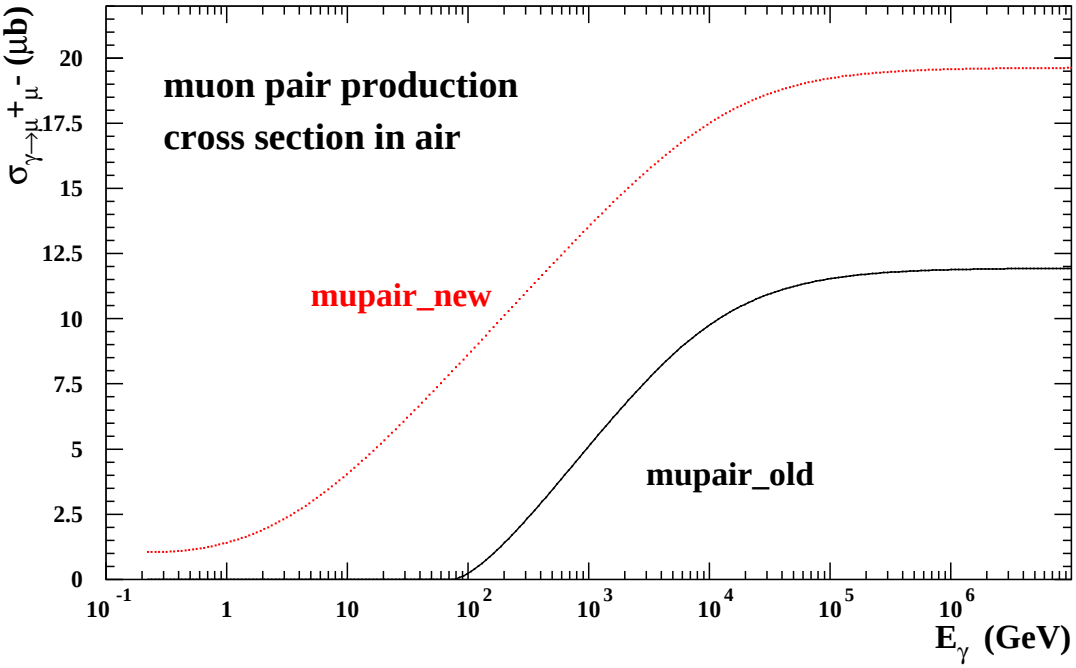

Figure 1: Old and new conversion cross sections in air as function of gamma energy

be performed over the complete range of transferred momentum, which at maximum is $\sim m_l$. Additionally the finite size of the nucleus has to be respected, as for the larger momentum transfer smaller collision parameters can be reached. The change in the upper boundary of this integral results finally in a higher cross section [7] of the $E_\gamma \rightarrow \mu^+ + \mu^-$ conversion which is increased by a factor of $\sim \log(m_\mu/m_e)$ thus lifting the saturation cross section from 11.4 μb (old treatment) to 19.6 μb (new treatment) as shown in Fig. 1.

3 Energy Distributions of Muons

The new treatment of the $E_\gamma \rightarrow \mu^+ + \mu^-$ conversion follows closely the proposed procedure of Ref. [6] which is realized in the `G4GammaConversionToMuons` routine implemented in the GEANT 4 Monte Carlo code [8]. The detailed description how to share the energy between the two created muons produces a modified energy distribution which is shown in Fig. 2 for a gamma energy of 1 TeV. The old treatment reflects the energy partition as expected for an e^+e^- pair. Because of the higher muon mass (relative to that of electrons) extreme asymmetric energy partitions are clearly suppressed in the new treatment. This suppression is most pronounced at low gamma

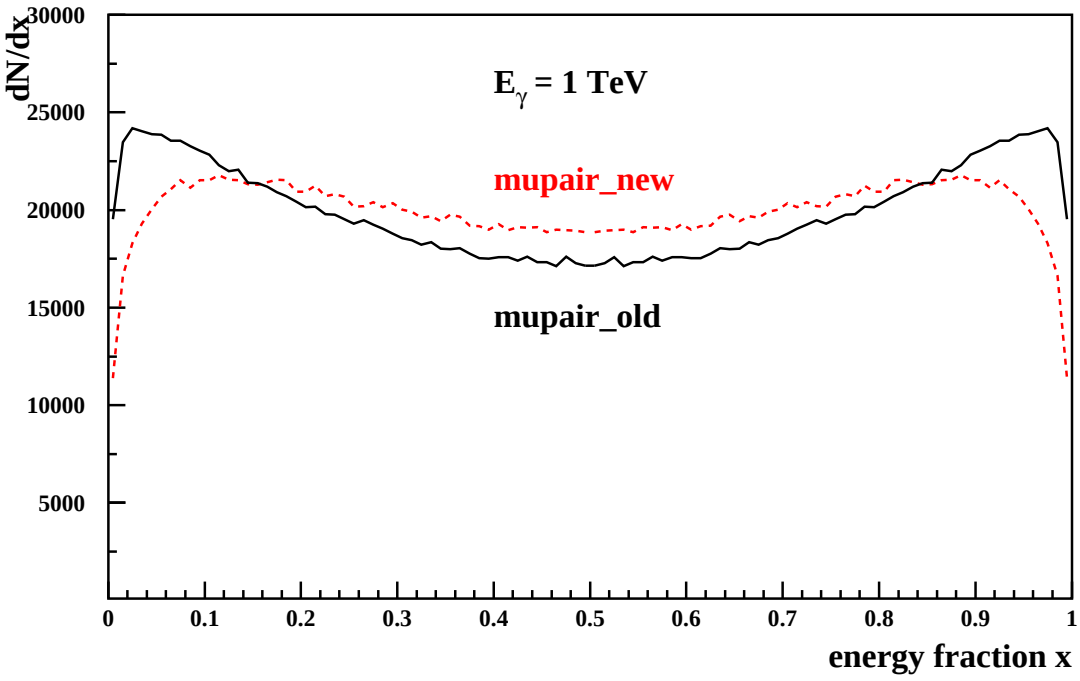

Figure 2: Energy distributions of muons from the conversion $\gamma \rightarrow \mu^+ + \mu^-$ in air at the gamma energy $E_\gamma = 1$ TeV. Both curves for old and new treatment of pair conversion are normalized for equal number of events.

energies and disappears more and more with increasing gamma energy. In Ref. [6] nice examples are given in its Figs. 2 and 5.

4 Angular Distributions of Muons

The calculation of the polar angles of the leptons in the $\gamma \rightarrow e^+ + e^-$ pair production is rather simplified in the EGS4 program [4] as the lateral distribution of the electromagnetic particles is anyway dominated by the multiple scattering of the electrons. Thus the polar angle Θ for both particles has been assumed to $\Theta = m_e/E_\gamma$, irrespective of the energy fractions of the emerging electrons and positrons. It should be remarked, that the values of the angle Θ are rather small as $E_\gamma \gg m_e$. To keep the analogy to the electron pair production this polar angle calculation has been maintained for the old version of the muonic pair conversion, just replacing the electron mass by the muonic one, which results in equal polar angles for both muons disregarding their energy partitioning.

In the new treatment of the $\gamma \rightarrow \mu^+ + \mu^-$ conversion both polar angles are calculated much more accurate with the prescriptions of Ref. [6] considering how the gamma energy has been partitioned between both muons. The resulting distributions of the muon polar angles are shown in Fig. 3, separately for the muons with the higher

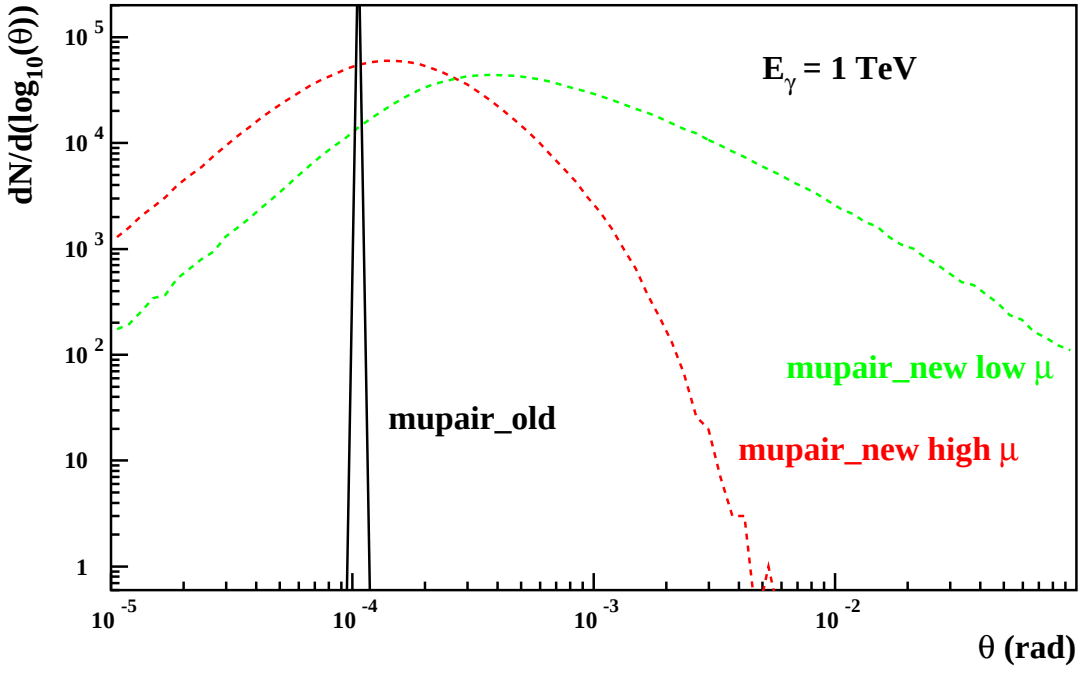

Figure 3: Polar angle distributions of muons from the conversion $\gamma \rightarrow \mu^+ + \mu^-$ in air at the gamma energy $E_\gamma = 1$ TeV.

energy (energy fraction x $>$ 0.5) and with lower energy (energy fraction x $<$ 0.5).

In the old treatment the azimuth angles are distributed uniformly, but with opposite directions for both muons. The new treatment [6] is much more precise by a more sophisticated calculation respecting the nuclear recoil which gives rise to a slight deviation from the exact opposite azimuth angle for the two muons.

5 Comparison of Muon Distributions from Showers

To demonstrate the influence of the different treatments of the $\gamma \rightarrow \mu^+ + \mu^-$ conversion, four sets of air showers have been generated using CORSIKA [9] with the options 'THIN', 'PRESHOW', 'EHISTORY', and 'AUGERHIST', the latter two have slightly been modified to discriminate muons produced by gamma conversion from all other

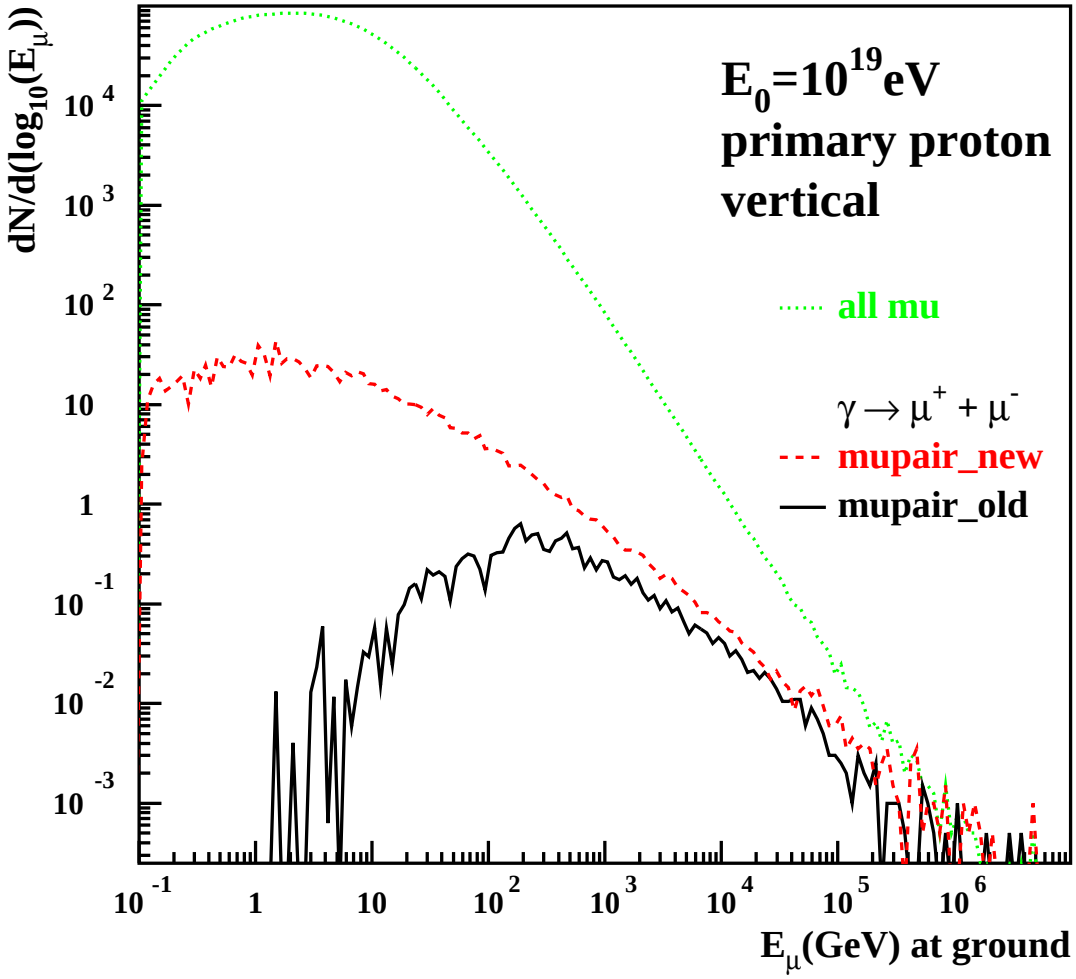

Figure 4: Energy distributions of muons from air showers with $E_0 = 10^{19}$ eV induced by vertically incident protons.

muon sources and to fill them into separate histograms for subsequent plotting. In each run 100 showers induced by primary particles of 10^{19} eV with vertical incidence have been started. The high-energy hadronic interactions are modeled with the QGSJET01 program [10], while the low-energy interactions are treated by the GHEISHA code [11] with improved kinematics [12]. The two sets with primary protons but with different treatment of the $\gamma \rightarrow \mu^+ + \mu^-$ conversion are compared in Fig. 4, while in Fig. 5 the results of the two sets with primary gamma (with possible preshowering [13]) are displayed.

The total number of muons per shower coming from $\gamma \rightarrow \mu^+ + \mu^-$ conversions amounts to ≈ 125 (new) vs. ≈ 25 (old) for the proton-induced showers. In the new treatment much more muons at energies below 100 GeV arrive at the detector level, caused by the much higher cross section at energies below 1 TeV (see Fig. 1). More-

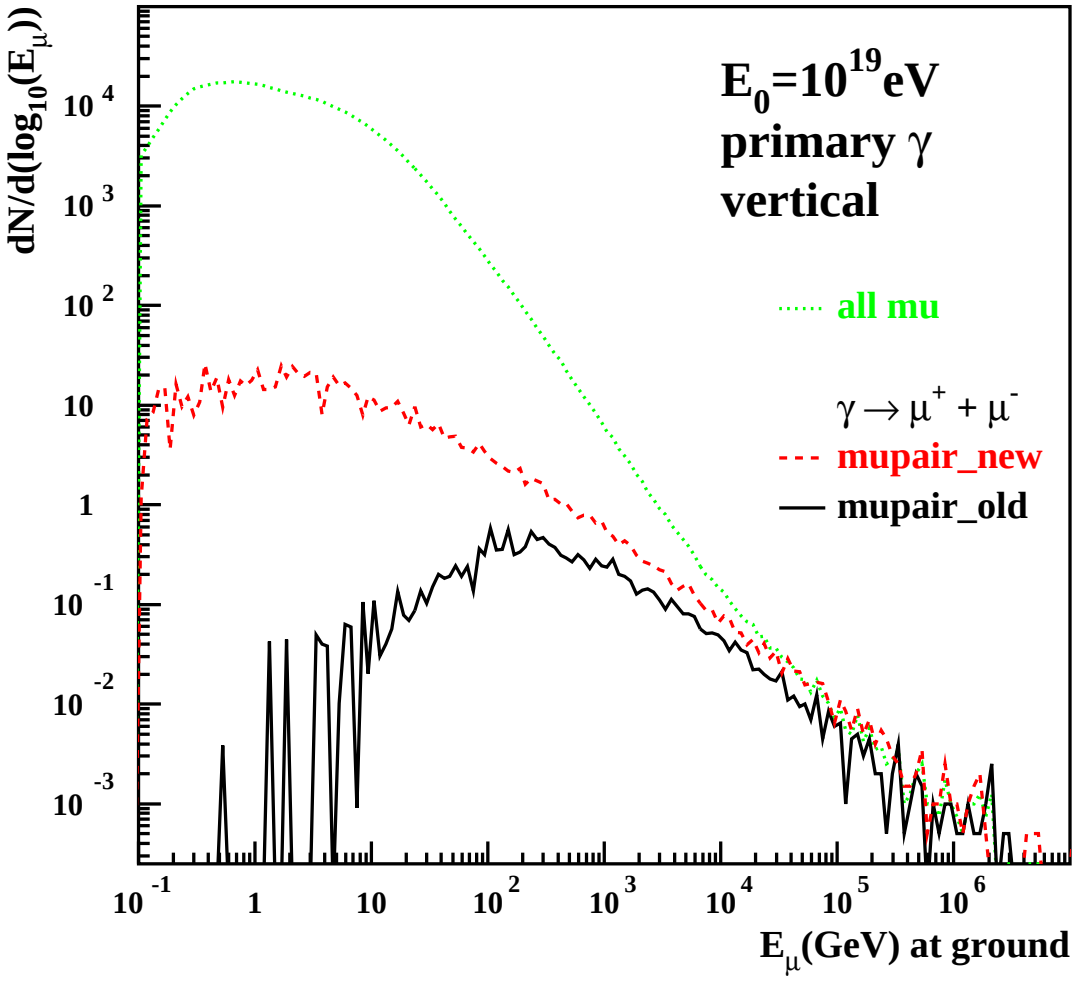

Figure 5: Energy distributions of muons from air showers with $E_0 = 10^{19}$ eV induced by vertically incident gammas.

over the increase of the muons with energies above 1 TeV has to be attributed to the higher saturation cross section at the highest gamma energies. For primary gammas the effect is very similar, the essential difference is the lower number of all muons (by a factor of ≈ 15), as much less muons are produced by decaying charged pions and kaons.

6 Other Rare Muon Production Processes

In this section other processes of em-particles leading to the production of $\mu^+\mu^-$ pairs are considered. These processes are too scarce to influence the behaviour of an extensive air shower and they are therefore not implemented in CORSIKA. Their contribution to the muons arriving at ground is negligible also at the highest energies as observed in the Auger experiment [14]. In Fig. 6 the cross sections for the two annihilation processes $e^+ + e^- \rightarrow \mu^+ + \mu^-$ and $e^+ + e^- \rightarrow Z^0$ are displayed together with that of the improved $\gamma \rightarrow \mu^+ + \mu^-$ conversion.

6.1 Annihilation to Muon Pair

The annihilation of a positron to a $\mu^+\mu^-$ pair is posssible above the threshold energy $E_{th} = 2m_\mu^2/m_e - m_e \approx 43.69$ GeV where m_μ and m_e are the muon and electron rest

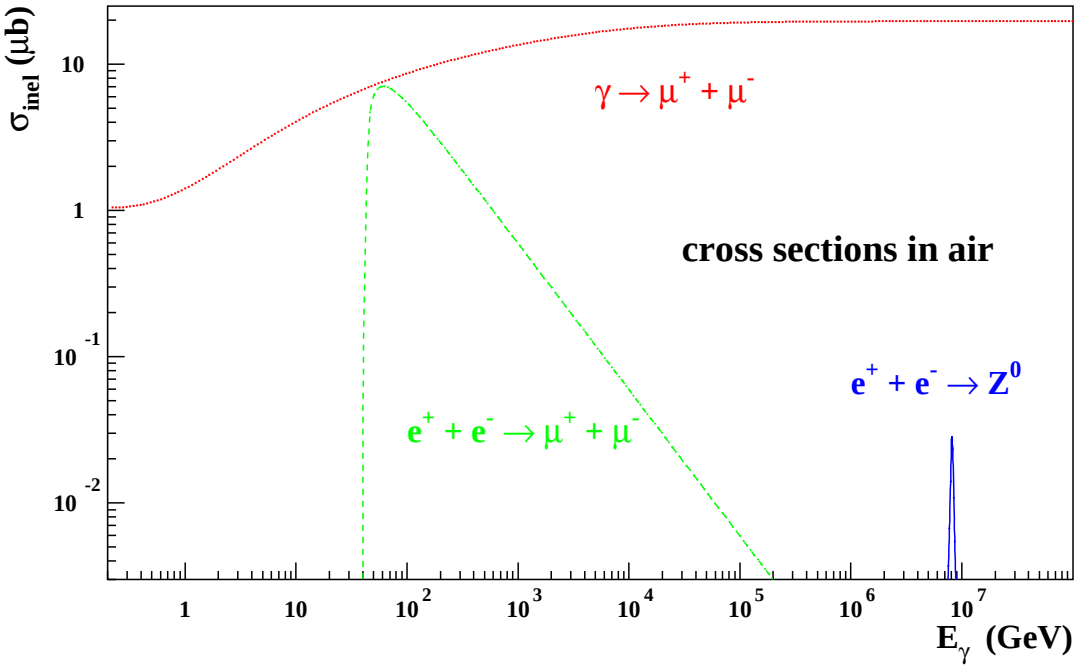

Figure 6: Cross sections in air for several rare processes which lead to the production of muons.

masses, respectively. The energy dependence of this cross section follows [15] the function

$$\sigma = \frac{\pi\, r_\mu^2}{3}\, \xi\, (1+\xi/2)\, \sqrt{1-\xi} \qquad (1)$$

where r_μ is the classical muon radius and $\xi = E_{th}/E$, with E the total positron energy in the laboratory frame. In Eq. 1 approximations are made by neglecting terms with $m_e^2 \ll m_\mu^2$. This function shows a maximum at $E = 1.396\, E_{th} \approx 60.99$ GeV, see Fig. 6.

As the total number of muons is proportional to the convolution of the local energy spectrum of the considered electromagnetic particles with the $\mu^+\mu^-$ pair production cross section, the annihilation $e^+ + e^- \rightarrow \mu^+ + \mu^-$ certainly is of much lower importance than the $\gamma \rightarrow \mu^+ + \mu^-$ conversion. The minor importance of this annihilation is further reduced by the lower number of positrons (compared with gammas of the same energy) in an air shower: They are less abundant by a factor $\geq$ 3 than the number of gammas in the energy range above ≥ 40 GeV, rather independent of the stage of shower development, see Figs. 14 and 15 of Ref. [16].

6.2 Annihilation to Z^0-Boson

Another annihilation to be considered is the production of a Z^0-boson, similar to its production in the e^+e^--collider LEP at CERN. Details of the Z^0-resonance parameters are given in Ref. [17]. In the laboratory frame the width of this narrow resonance at $\approx$ 8136 TeV amounts to FWHM $\approx$ 446 TeV. This resonance decays, besides the hadronic channels, into lepton pairs. The branching ratio for the decay $Z^0 \rightarrow \mu^+ + \mu^-$ amounts only to 3.366% [18]. As a consequence in air showers its contribution to the muons arriving at ground is negligible because of the low cross section (see Fig. 6) in combination with the low branching ratio.

7 Final Remarks

The updated version 6.960 of CORSIKA contains the new treatment of the gamma conversion to a muon pair $\gamma \rightarrow \mu^+ + \mu^-$ as described in Sect. 2. Because of the modified cross section also the tables contained in the cross section files for the electromagnetic processes have been recalculated. To ascertain a correct use of the updated CORSIKA with the new cross section files they have been renamed to EGSDAT6_x.x.

Because of the minor importance to the production of muons the annihilation processes described in Sect. 6 have not been implemented in the EGS-routines of the updated CORSIKA version. But suitable routines have been added to the (modified) PEGS4 program [4] which calculates the cross sections and branching ratios for the various processes of the em-particles.

References

[1] J.N. Capdevielle et al., Report **KfK 4998**, Kernforschungszentrum Karlsruhe (1992)

[2] T. Stanev and Ch.P. Vankov, *Phys. Lett.* **158 B** (1985) 75

[3] D. Heck et al., *CORSIKA: A Monte Carlo Code to Simulate Extensive Air Showers*, Report **FZKA 6019**, Forschungszentrum Karlsruhe (1998); http://www-ik.fzk.de/corsika/physics_description/corsika_phys.html

[4] W.R. Nelson, H. Hirayama and D.W.O. Rogers, Report **SLAC 265**, Stanford Linear Accelerator Center (1985)

[5] A. Ò Murchadha (University of Wisconsin, Madison), private communication (2009)

[6] H. Burkhardt, S.R. Kelner, and R.P. Kokoulin, Report **CERN-SL-2002-016 (AP)**, European Organization for Nuclear Research (2002)

[7] F. Halzen, A. Kappes, and A. Ò Murchadha, preprint arXiv:0909.3836 [astro-ph.HE] (2009)

[8] GEANT4 home page http://geant4.web.cern.ch/geant4, Physics reference manual http://geant4.web.cern.ch/geant4/UserDocumentation/UsersGuide/PhysicsReferenceManual/fo/PhysicsReferenceManual.pdf

[9] D. Heck and T. Pierog, *Extensive Air Shower Simulation with CORSIKA: A User's Guide.* The actual version is available from http://www-ik.fzk.de/corsika/usersguide/corsika_tech.html

[10] N.N. Kalmykov, S.S. Ostapchenko, and A.I. Pavlov, *Nucl. Phys. B* (Proc. Suppl.) **52B** (1997) 17

[11] H. Fesefeldt, Report **PITHA-85/02**, RWTH Aachen (1985)

[12] R.E. Cassell and G. Bower (SLAC), private communication (2002)

[13] P. Homola et al., *Comp. Phys. Comm.***173** (2005) 71; arXiv:0311442 [astro-ph] (2003)

[14] J. Abraham et al. (Pierre Auger Collab.), *Nucl. Instr. Meth.* **A523** (2004) 50

[15] H. Burkhardt, S.R. Kelner, and R.P. Kokoulin, Report **CERN-AB-2003-002 (ABP)**, European Organization for Nuclear Research (2003)

[16] D. Heck and M. Risse (P. Auger Collab.), talk presented (in German) at the Spring Meeting of the German Physical Society, Leipzig (Germany) March 18 - 22 (2002) available from http://www-ik.fzk.de/~heck/publications/

[17] G. Duckeck et al., Report **CERN-EP-2000-153**, European Organization for Nuclear Research (2000); preprint arXiv:0101027 [hep-ex] (2001)

[18] C. Amsler et al. (Particle Data Group), *Phys. Lett.* **B667** (2008) 1